A REVIEW OF THE ARROW FLUTTER

PROGRAM

AVRO AIRCRAFT

The Correlation of Theory and Model Test Results In the Flutter Clearance Program of the Arrow

(1) This report is a discussion of the theories that were used in the flutter work on the Arrow and their correlation with tests of flutter models. First, the work on the fin will be discussed and later the work on the wing. Finally, some thoughts on future problems, associated with the design, will be briefly treated.

(2) The fin was treated structurally as a swept beam. Even though the aspect ratio was low, the large percentage rudder made this treatment quite a reasonable proposition. Three modes of vibration were calculated by the Targoff matrix method. These three degrees of freedom, together with rudder flapping were used in the flutter analysis.

The aerodynamic treatment was the velocity component strip method (1) using incompressible derivatives with corrections for taper and for the spanwise flow component. Several rudder rotation frequencies were used in the analysis to assess the influence of control circuit stiffness on the flutter characteristics. The results are shown in figure (2). The flutter speed rises with rudder frequency then the mode alters to flexure-torsion. Above 20,000 ft. there is no flutter. In 1956 the company was advised by WADC that tests had shown that a rudder frequency of 70% of the torsion frequency was required. Accordingly, when the flutter model was built provision was made for testing a complete range of rudder frequencies.

Cont'd...../2

A summary of the model parameters is given in table I and the model flutter points compared with theory in figure (3). A strip print showing one cycle of flutter just before failure is shown in figure (4). Generally good agreement was obtained with the model results showing higher speeds. The rudder flutter mode was seen to disappear as rudder frequency was raised higher than the fin bending frequency and this effect has been confirmed by recent conversations with WADC.

To assess the Mach number effects on flutter the flight envelope and low speed model results were plotted on a non dimensional chart with NACA results for similar surfaces. Since the margin was so high, no transonic model tests were considered necessary. Supersonic calculations using modified two dimensional derivatives showed no flutter and the fin was considered cleared.

(3) The wing was treated as a plate because of the low aspect ratio. The vibration modes were calculated by the matrix-iteration method from a 60 point matrix. The frequencies turned out to be quite low and it was decided to include all wing modes up to the anticipated control surface frequencies. This required the inclusion of six modes. Since the vibratiom analysis had considered the aircraft as a free body, pitch and translation were not included in the analysis as separate degrees of freedom, as it was felt they were incorporated into each mode.

Cont'd...../3

The aerodynamic treatment followed two different lines. First a strip theory using incompressible derivatives and chordwise strips with the quarter chord line as reference axis. Secondly, the strip theory was modified according to the rules set forth by Minhinnick (2) and thirdly, an extension was made of Lawrence and Gerber's theory to provide surface derivatives over the wing at the mode points of the vibration analysis. (3) Cantilever, symmetric full airplane and antisymmetric full airplane analyses were made. The results of the various approaches are seen in fig. (6&7) As with the fin and rudder, a range of elevator and aileron frequencies were covered.

In discussions at WADC and Cornell on the Arrow flutter program, the non-dimensionalized flutter curve of fig. (8) was obtained. Since the Arrow sea level performance line plotted on the same basis showed little margin, it was decided to build a flutter model to check the accuracy of the calculations. Summaries of the cantilever wing and the full airplane model parameters appear in tables II and III. Results of the cantilever wing-aileron tests are shown in fig. (9) and of the full airplane in fig. (11). These results showed the calculations to be conservative.

Cont'd...../4

Calculations were carried out at supersonic speeds for both cantilever and symmetric full airplane cases. These showed little margins in the transonic range, but the actual curve was not clear. The theory was strip theory with the derivatives modified for taper but not for leading edge sweep. Accordingly, transonic models were built and tested to provide more adequate coverage of this uncertain range. The results are shown in figs. (14 and 15) compared with the calculations. They show the marked influence of frequency ratio between the first and second modes in the cantilever case. The improved margin over that calculated is also seen. This margin is quite large. In the full airplane case the margin is not so marked. Fortunately the ground resonance tests showed that the frequency of the second mode was considerably higher and this provides an improved margin.

(4) Other problems and projected work.

4.1 Control Surface Buzz

Calculations in one degree of freedom show a region of negative damping of the three controls at a Mach number of about 1.25. Typical curves are shown for the elevator. As a result of this work provision was made on the first airplanes for buzz dampers. However, calculations with all wing or fin degrees of freedom included, indicate that this buzz condition will not occur. Model tests are difficult since this Mach number is about the operating limit for tunnels, and so measurements are difficult. Accordingly, this flight regime will be approached with caution during flight tests and dampings measured to establish clearance through this range.

Cont'd...../5

4.2 Autopilot System Flutter

The accelerometers and gyros of the autopilot system will, of course, sense airframe vibration and feed it into the system as a false signal. Since these signals will be in a frequency range that the system must accept, control surface movement will result. It is possible, if the design is not carefully arranged, to have this loop unstable. Work has been carried out to estimate the response of the sensors to steady elevator oscillation with a view to arrange sensor location to minimize these false signals. A typical plot is shown in fig. (19). These calculations will have to be confirmed by flight tests.

4.3 Ground Resonance Test Philosophy

In checking the calculations for the dynamic structural characteristics of the aircraft, the ground resonance test is one of the most important milestones. The problem of support for an aircraft the size of the Arrow is a considerable one. Since the test is primarily a check of calculations, the decision was made to provide a known support, and compute the vibration modes for this support. The three point suspension of the undercarriage was used and the associated modes computed. Comparison of results is shown in fig. (20)

Cont'd...../6

4.4 Remaining Work

Ground resonance test results have shown that the aircraft fuselage and wing are stiffer than calculations showed. On the other hand, the fin did not turn out quite so clearly. Considerable rudder torsion coupling was apparent in the third mode. A five degree of freedom analysis is now under way to clear this and the fin model is being altered to give the test case for checking in the tunnel. It is proposed to rework one wing which is relatively undamaged and retest it, but this is just in the nature of a formality.

REFERENCES

(1) USAF AMC MR MCREXA 5-4595-4 - Methods for calculating the flutter and vibration characteristics of Swept wings at subsonic speeds.

(2) RAE Technical Note Structures 185. Flutter prediction in practise.

(3) Second Canadian Symposium on Aerodynamics (Feb '54) "Lift and Moment of Low Aspect Ratio Wings in Incompressible Unsteady Flow".

Cont'd...../7

Discussion of Films

Low speed model construction is pretty clearly shown. Instrumentation consisted of:-

Fin - bending and torsion strain gages.

- rudder rotation strain gage.

Wing - 4 accelerometers

- 2 bending and 2 torsion strain gages.

- elevator and aileron strain gages.

Complete aircraft - 4 fuselage accelerometers

- 2 strain gages.

The accelerometers were specially made barium titanite type. The main problem is that they are extremely good microphones. It proved difficult to filter out noise and other undesired signals.

An electromagnetic exciter was used to attempt to excite the model frequencies during testing. This did not work adequately as the exciter force was swamped by tunnel turbulence. (See sweeps in fig. 22).

The Dutch roll arises from the fact that the fin aeroelastic effects are magnified by a factor of 5. This loss in directional stability was not representative of full scale aircraft conditions. The solution had to have no effect on the fuselage bending mode.

Cont'd...../9

The pitching instability arises from the restraint in the fore & aft directions combined with the finite frequency in vertical translation. If the spring had been omitted there would have been no trouble. However, it was felt better to have the spring to allow testing at $C_L = 0$ and provide the pitching restraint.

No antisymmetric flutter was obtained, even when only one aileron was free.

Transonic Tests.

The models had a skin thickness of 2.5 to 3 thousandths of an inch. The core was end grain balsa. The leading and trailing edges were balsa with pine reinforcement. The skin was bonded to the core by punching the skin and pressing plastic aluminium into the hole to form a sort of rivet. The skins were tapered by chemical milling.

The amazing result of the transonic test was the relatively mild form of flutter. Even with damping of the order of 1.5% no model was broken. Peak dynamic pressure in the tunnel was 8.5 psi. which is no mean pressure.

Instrumentation consisted of bending and torsion strain gages on each wing root.

TABLE I

Stiffness Test

Bend moment - 1 lb. applied at station 180.

STATION	CALC. SLOPE	TEST SLOPE	RATIO	EI RATIO
1.875	1.77×10^{-6}	$.908 \times 10^{-2}$	$.513 \times 10^{4}$	513
5.453	5.64×10^{-6}	2.945×10^{-2}	.522	522
9.656	11.38×10^{-6}	5.285×10^{-2}	.465	465
13.875	18.22×10^{-6}	8.24×10^{-2}	.451	451
17.75	22.55×10^{-6}	10.37×10^{-2}	.460	460
			MEAN	482

Torque Applied - 1 in lb applied at station 180.

STATION	CALC. θ	TEST θ	RATIO	CJ RATIO
1.875	$.0052 \times 10^{-6}$	.000413	$.795 \times 10^{5}$	795
5.45	.0180	.00177	.983	938
9.66	.0452	.00421	.932	932
13.875	.1025	.00898	.875	875
17.75	.2183	.02005	.920	920
			MEAN	901

Vibration Tests

MODE	CALC. FREQ.	TEST FREQ.	RATIO
1	7.63	11.2	1.470
2	28.87	39.8	1.380
3	30.82	40.9	1.326
		MEAN	1.393

Summary of Fin Tests

Stiffness ratio $\delta_m/\delta_F = .466$

Mass ratio $W_m/W_F = \frac{1.11}{1000}$

Frequency ratio $\omega_m/\omega_F = 1.400$

Length ratio $L_m/L_F = .10$

Speed Scale $V_m/V_F = 1/7.15$

The model fluttered in flexure-torsion at a speed of 302 ft/sec representing a speed of 2160 ft/sec at an altitude of 2000 ft.

WADC Flutter Criterim Applied to Fin

NACA Model - 45° Sweep on quarter chord.

Taper ratio = .39

= 1.66 on semispan

b_r taken at 75% semispan.

μ taken normal to quarter chord.

	Mach No.		
$\frac{V_E}{b_r \omega_\alpha \sqrt{\mu}}$	.8	1.05	1.2
$\mu = 20$	.55	.52	.65
$\mu = 90$	.55	.43	.65

C105 Fin

At elastic axis station 180 b_r = 3.178 ft.

m = 33.0 lb/ft.

ω_α = 193.5 rps

CosΛ = .65

H	$\pi\delta$	μ	$\sqrt{\mu}$	V_D	$\frac{V_D \cos\Lambda}{b_r \omega_\alpha \sqrt{\mu}}$
SL	.2404	13.61	3.69	1217	.348
10	.1775	18.44	4.30	1411	.347
20	.1280	25.60	5.06	1660	.346
30	.0898	36.55	6.05	1990	.348

Model

b_r = .318 m = .367 lb/ft

ω_α = 262 rps μ = 15.1

V_F = 302 ft/sec $\sqrt{\mu}$ = 3.89

$\frac{V_F \cos\Lambda}{b_r \omega_\alpha \sqrt{\mu}}$ = .605 M = .270

TABLE II

Tests and parameters of cantilever wing

(a) Low speed

Stiffness Test

Comparison of Influence co-efficients.

Low at Dept. At	23			30			37		
	Calc.	Exp.	Ratio	Calc.	Exp.	Ratio	Calc.	Exp.	Ratio
17	108.4×10^{-6}	.048	443	116.6×10^{-6}	.050	439	120.9×10^{-6}	.055	455
19	109.4	.048	439	173.7	.075	431	208.1	.095	456
28	202.5	.092	454	470.7	.220	467	625.2	.300	480
2[illegible]	102.4	.048	468	228.8	.110	480	303.7	.140	461
32	157.1	.072	458	405.4	.185	456	579.7	.265	457
39	239.7	.106	442	697.1	.305	437	1253.7	.490	390.5

The average factor on the influence co-efficients is 454.

Vibration Test

Mode	Calc. Freq.	Test Freq.	Ratio
1	3.79	6.3	1.661
2	8.75	14.5	1.655
3	9.83	17.0	1.729
4	15.11	20.8	1.374
5	15.81	27.8	1.756

Summary of Testing of Cantilever Wing

Stiffness ratio $\delta_m/\delta_W = 454$

Mass ratio $W_m/W_m = \frac{.763}{1000}$

Frequency ratio $\omega_m/\omega_W = 1.700$

Length ratio $L_m/L_W = .10$

Speed Scale $V_m/V_W = 1/5.89$

Using this scaling, the model fluttered at 243 ft/sec representing a speed of 1430 ft/sec at an altitude 8700 ft. below sea level.

WADC Flutter Speed - Mach number Curve

Ordinate is a flutter speed coefficient $\frac{V_F}{b_r \omega_\theta \sqrt{\mu}}$

V_F = flutter speed (ft/sec)

b_r = root semi-chord (ft)

ω_θ = torsion frequency. (rad/sec) cantilever

μ = wing weight $/\pi \rho \int b^2 dx$

Application to C105

Chord at edge of fuselage = 445" b = 18.54' = b_r

Chord at tip = 52.8" b = 2.20'

Semi span is 20'

$\int b^2 dx$ = 3000 ft^3 wing weight = 8181 lb. ω_θ = 55.0 rps (8.75 cps)

TABLE II Cont'd

H	πS	μ	$\sqrt{\mu}$	V_D	$\frac{V_D}{b_r \omega_\theta \sqrt{\mu}}$
S.L.	.2404	11.32	3.36	1217	.3545
10,000	.1775	15.35	3.92	1411	.3530
20,000	.1280	21.30	4.61	1660	.353
30,000	.0898	30.35	5.50	1990	.3545

Application of WADC criterion to model.

ω_θ = 91.1 rps

μ = 8.65 $\sqrt{\mu}$ = 2.94

b_r = 1.85

$$\frac{V_F}{b_r \omega_\theta \sqrt{\mu}} = .488$$

(b) Tests and parameters of Transonic models

Coefficient is $\frac{V_F}{b_r \omega_\theta \sqrt{\frac{M}{\pi S \int b^2 dx}}}$ and can be rewritten as $\frac{1}{b_r \omega_\theta} \sqrt{\frac{2\pi \int b^2 dx \; q_F}{M}}$

Thus each tunnel run gives a line on the Mach number chart to compare with the flight envelope and criteria.

Model Frequencies

Calculated Frequency Model No.	3.79		8.75		9.83		15.11		15.81	
4	142	(37.5)	366	(41.8)	397	(40.4)	456	(30.2)	565	(35.7)
4 (cut skin)	137	(36.2)	339	(38.8)			443	(28.65)	511	(32.3)
1	120	(31.65)	318	(36.35)			393	(26.0)	500	(31.6)
1 (cut skin)	118	(31.1)	301	(34.4)			385	(25.5)	484	(30.6)
2 (cut skin)	127	(33.5)	290	(33.2)			369	(24.4)	470	(29.7)
5	114	(30.1)	290	(33.2)			395	(26.1)	459	(29.0)
5A	115	(30.3)	276	(31.5)			388	(25.7)	445	(28.2)
[illegible]	114	(30.1)	260	(30.8)			380	(25.2)	441	(27.9)
6	118	(31.1)	272	(31.1)	292	(29.7)	353	(23.4)	440	(27.8)

The mass of the models is difficult to measure, but, taking a mass of 33 grams as a reasonable figure, the criterion lines may be calculated from the tunnel characteristic.

TABLE III

Complete Airplane Tests and Parameters

Symmentric Modes.

	Test	Calc.	Ratio	
1.	6.35	4.36	1.453	
2.	8.25	5.88	1.403	
3.	16.30	10.08	1.617	1.541
4.	19.5	12.0	1.624	
5.	22.5	13.98	1.610	

Antisymmetric Modes.

	Test	Calc.	Ratio	
1.	9.5	5.45	1.745	
2.	12.9	7.58	1.702	1.685
3.	20.9	12.04	1.735	
4.	22.0	14.10	1.560	

Mean frequency ratio = 1.605

Since the primary flutter case is symmetric, the speed and time scale will be taken from the symmetric ratios.

Thus $V_m/V_F = 1/6.50$

The model collapsed at the onset of weak flutter at 216 ft/sec, representing 1402 ft/sec at sea level.

The model experimental point is plotted on the basis of mass ratio of 1000 and the mean frequency ratio.

(b) Correlation of transonic model tests and parameters.

Model Frequencies

	Translation 0	Pitch 0	4.36	5.88	10.08	12.0
7	43.5	71.5	130 (29.8)	238 (40.5)	335 (33.2)	360 (30.0)
8	45.5	71.0	137.0 (31.4)	248 (42.1)		385 (32.1)

As with the cantilever models, a mass of 33 grams is taken for the purpose of calculating criterion curves.

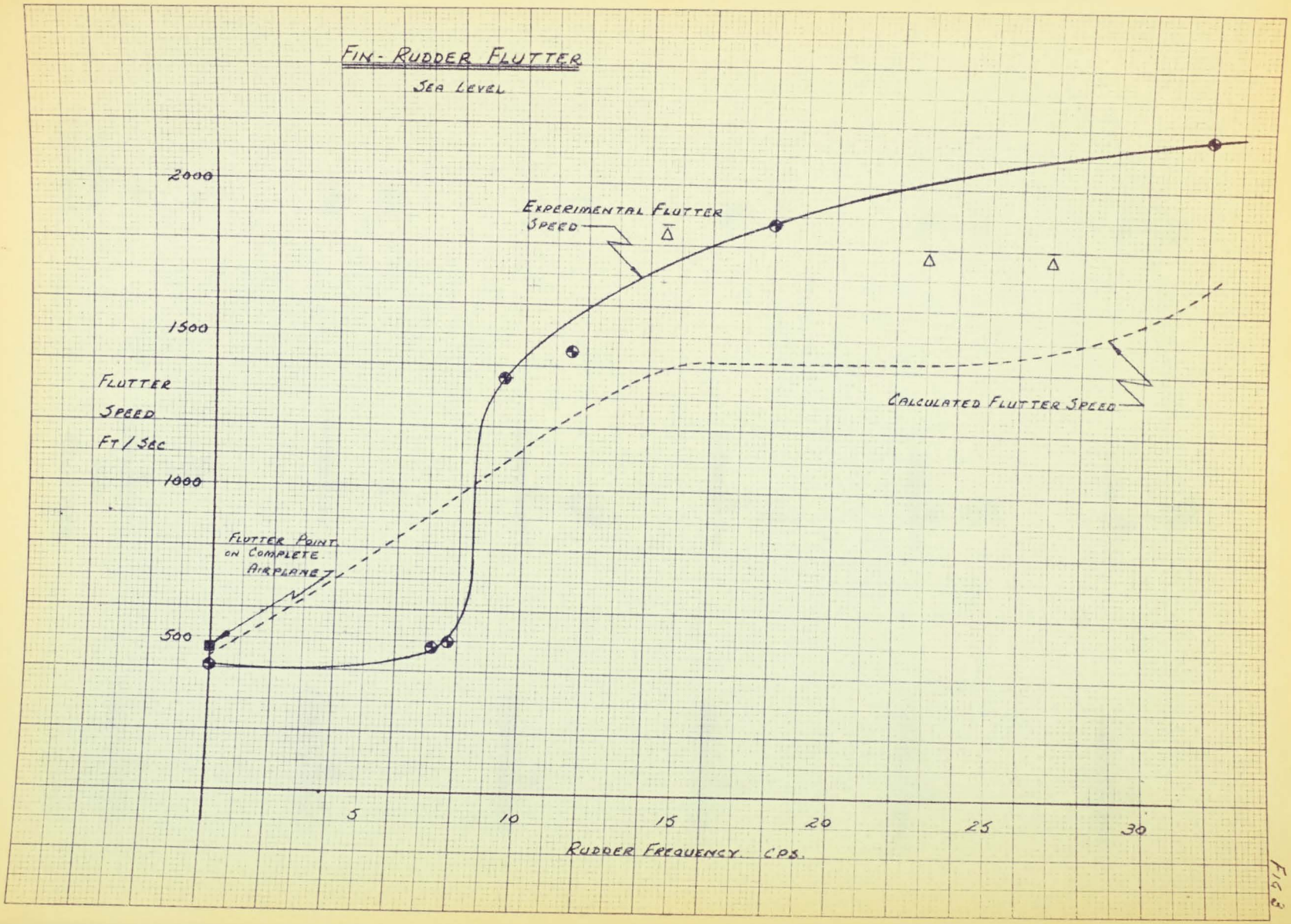

Fig 3

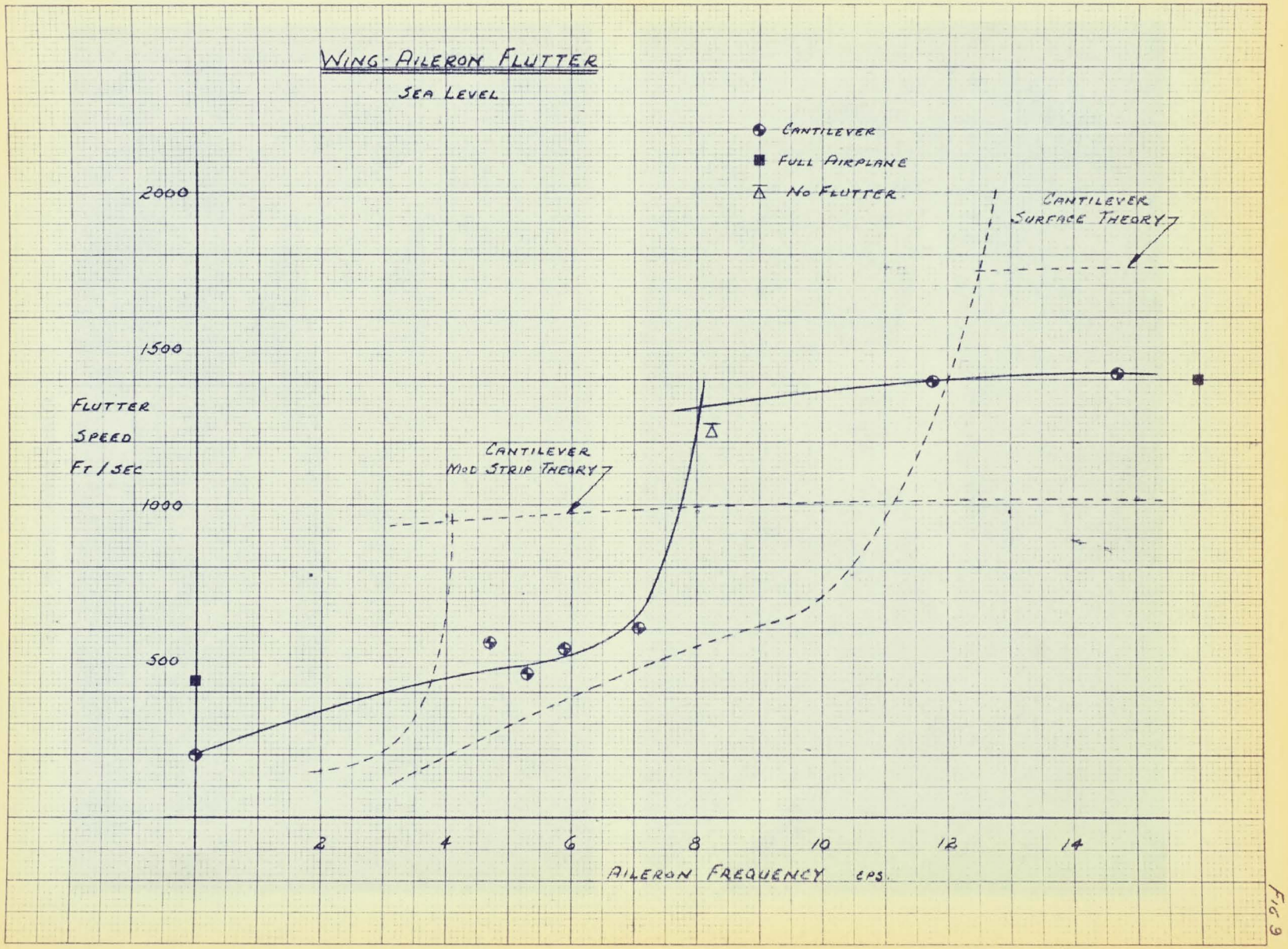

Fig 9

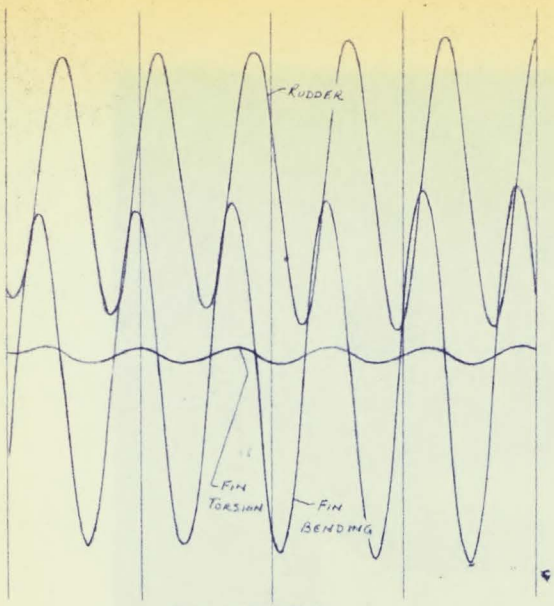

COMPONENT TEST
FREE RUDDER
9.9 CPS - FULL SCALE
400 FT/SEC - FULL SCALE

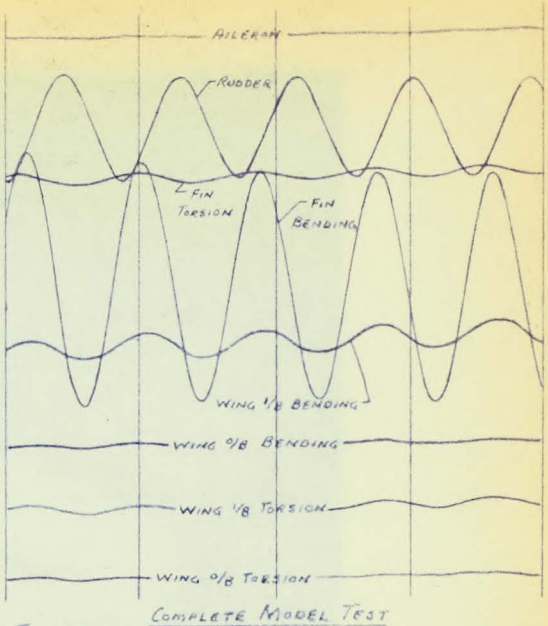

COMPLETE MODEL TEST
FREE RUDDER
7.5 CPS - FULL SCALE
468 FT/SEC - FULL SCALE

FIN - RUDDER FLUTTER

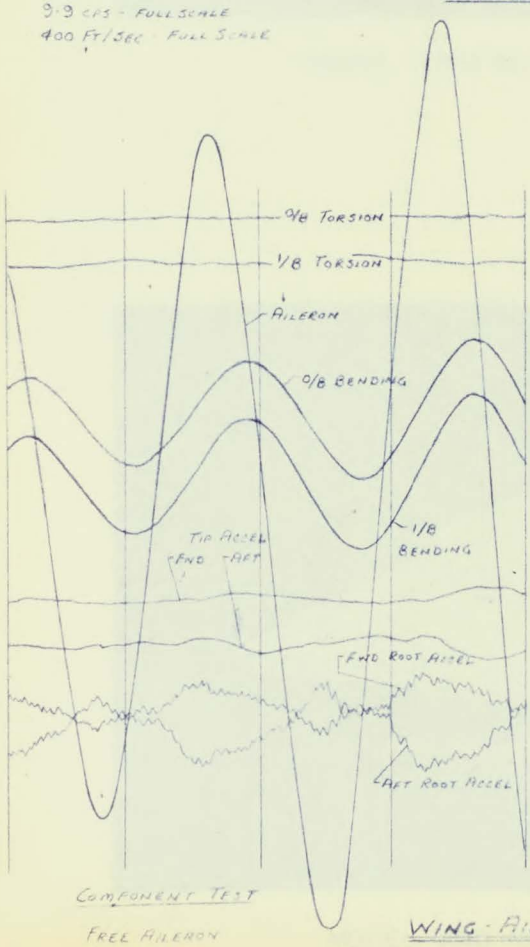

COMPONENT TEST
FREE AILERON
218 FT/SEC
3.56 CPS

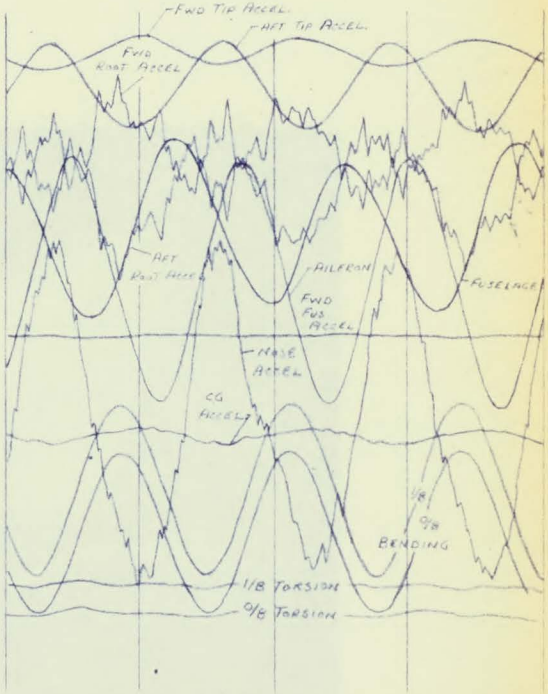

COMPLETE MODEL TEST
FREE AILERON
440 FT/SEC
5.98 CPS

WING - AILERON FLUTTER

TYPICAL FLUTTER RECORDS

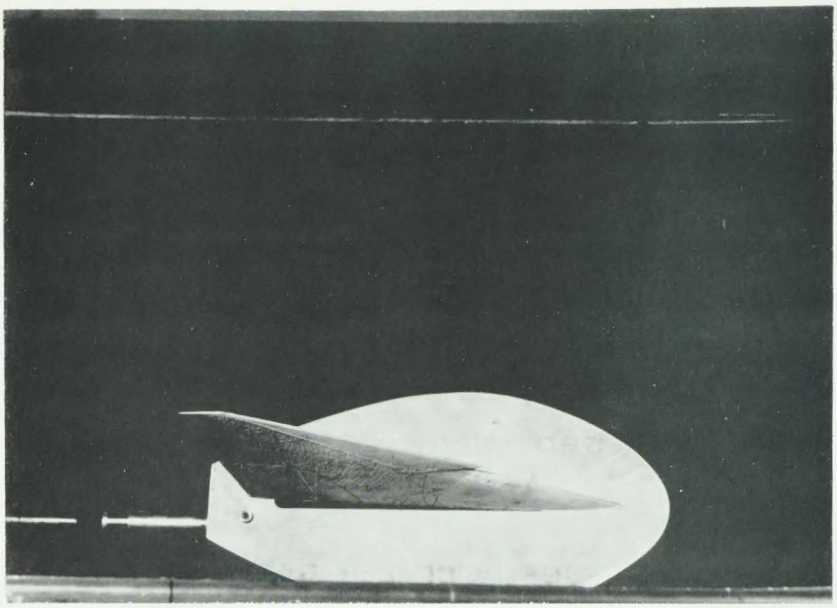

MODEL INSTALLED IN TUNNEL

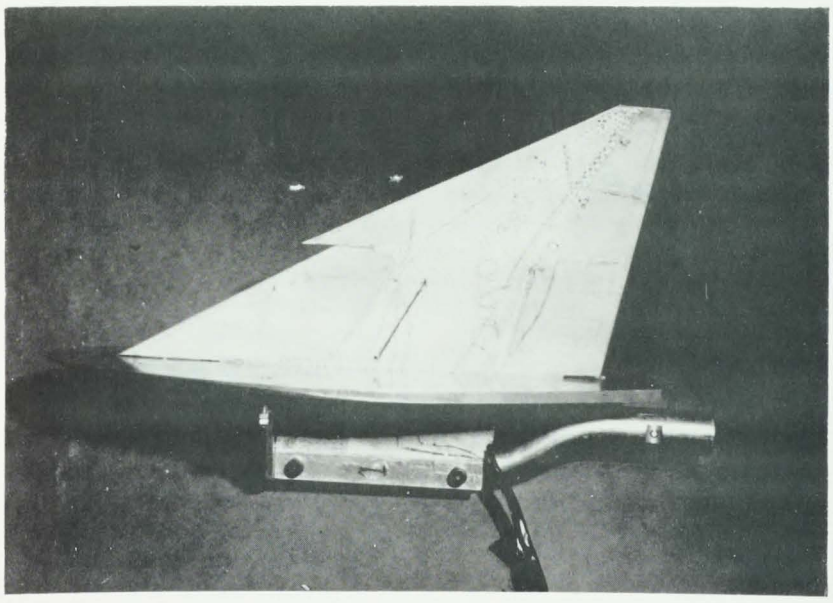

MODEL AND MODEL MOUNT

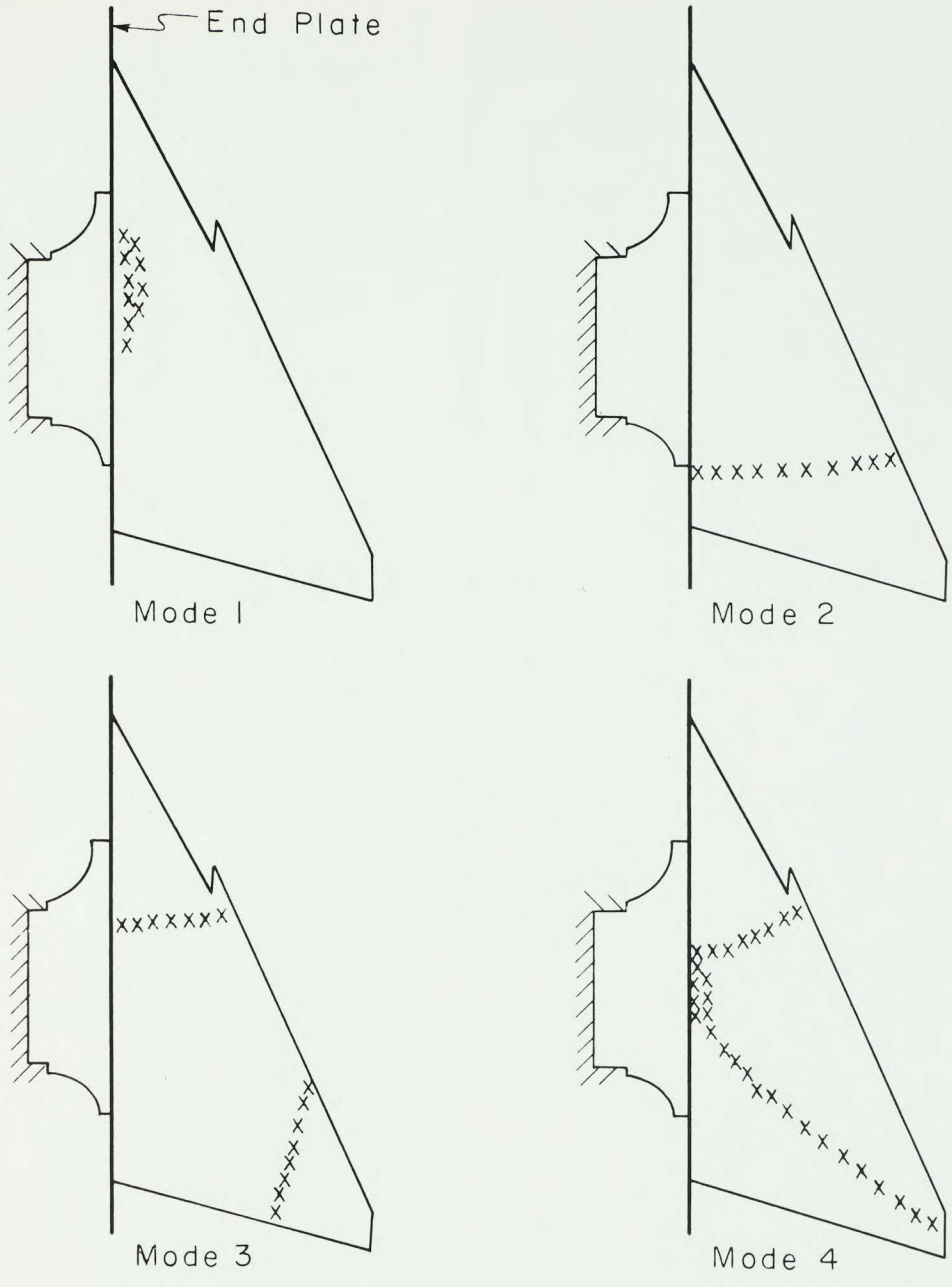

NODE LINES FOR FIRST FOUR VIBRATION MODES. TYPICAL OF ALL MODELS TESTED.

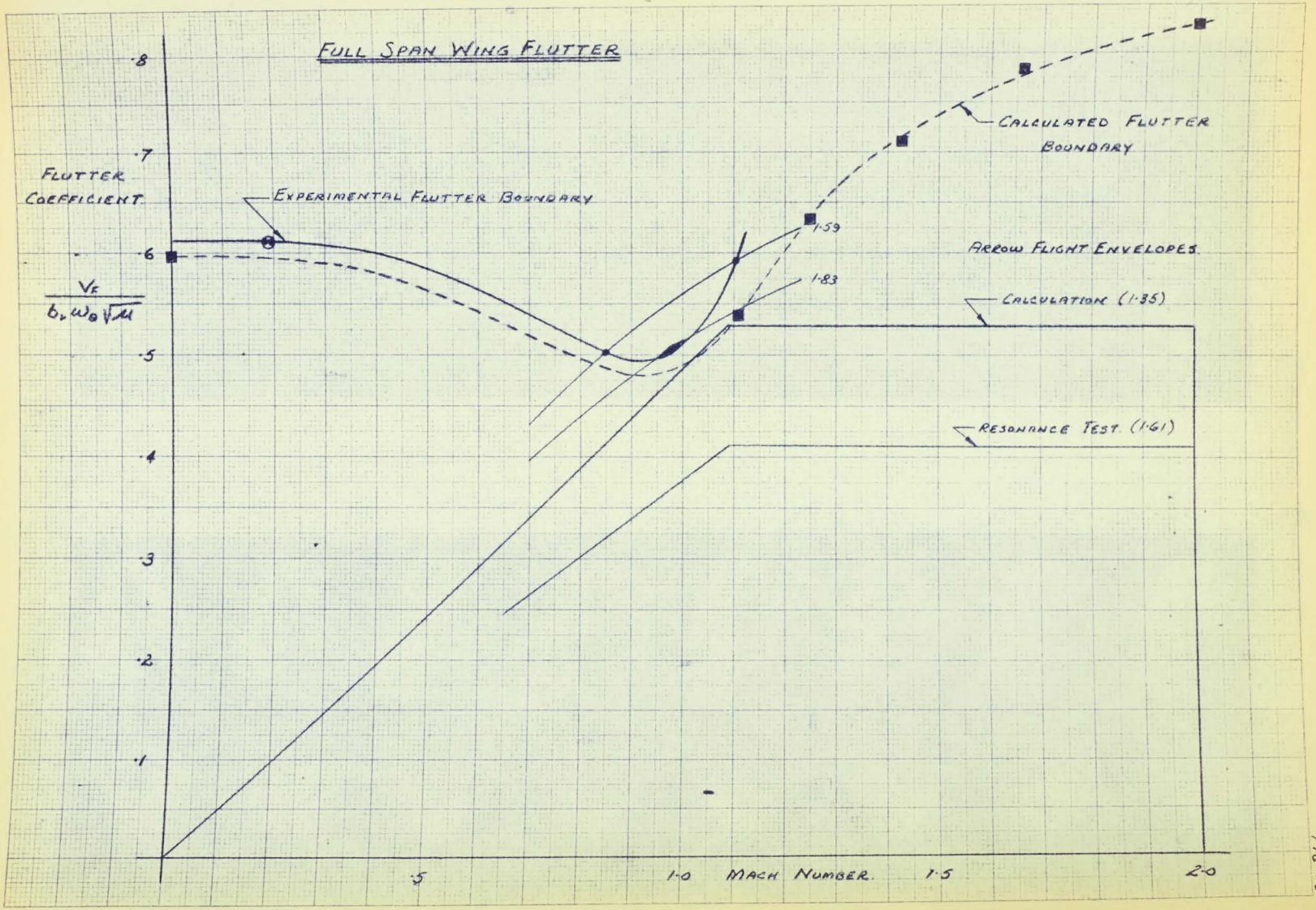

FIG 15

TRANSONIC FLUTTER

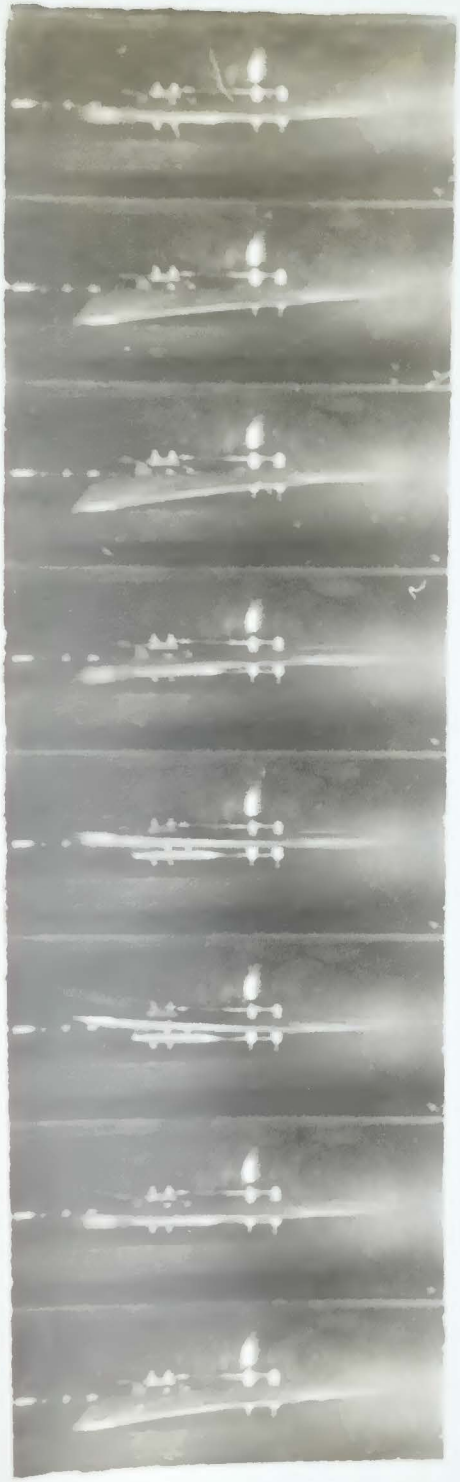

FULL SPAN

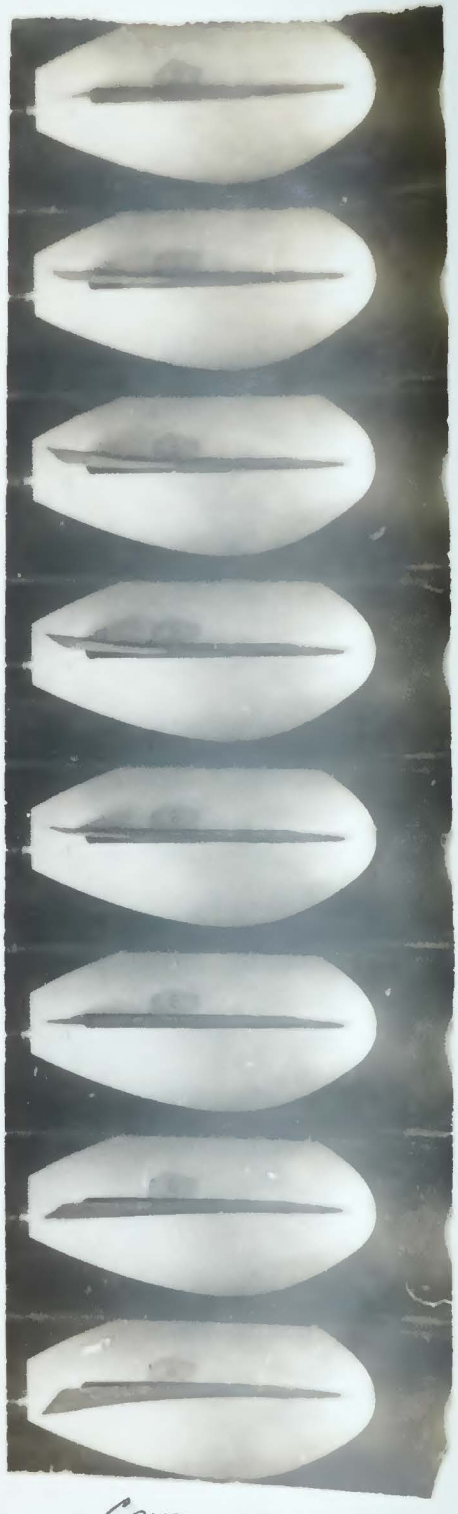

CANTILEVER

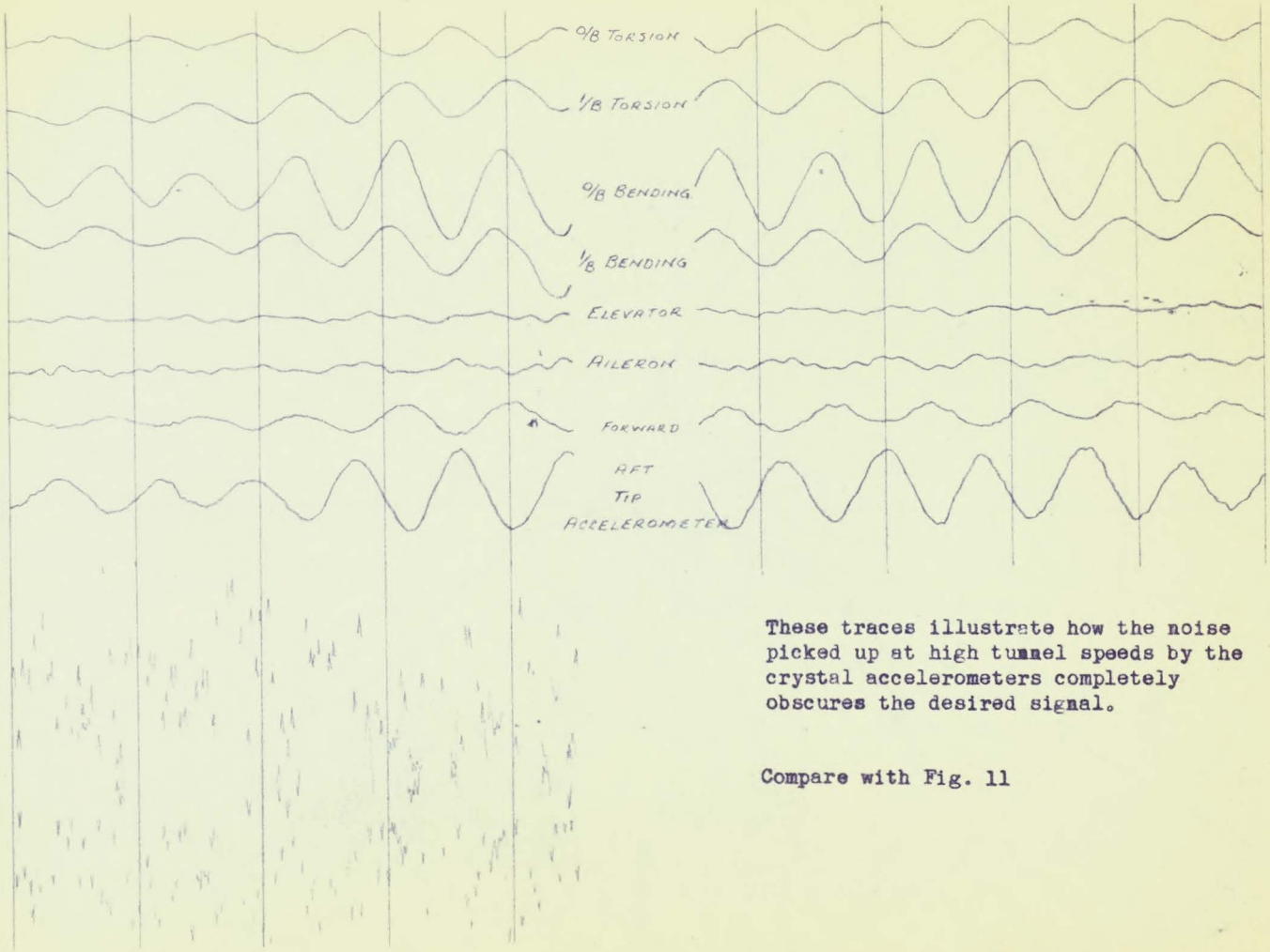

WING FLUTTER RECORD

6.5 SEC

1395 FT/SEC FULL SCALE

These traces illustrate how the noise picked up at high tunnel speeds by the crystal accelerometers completely obscures the desired signal.

Compare with Fig. 11

FIG 18

FIG. 19

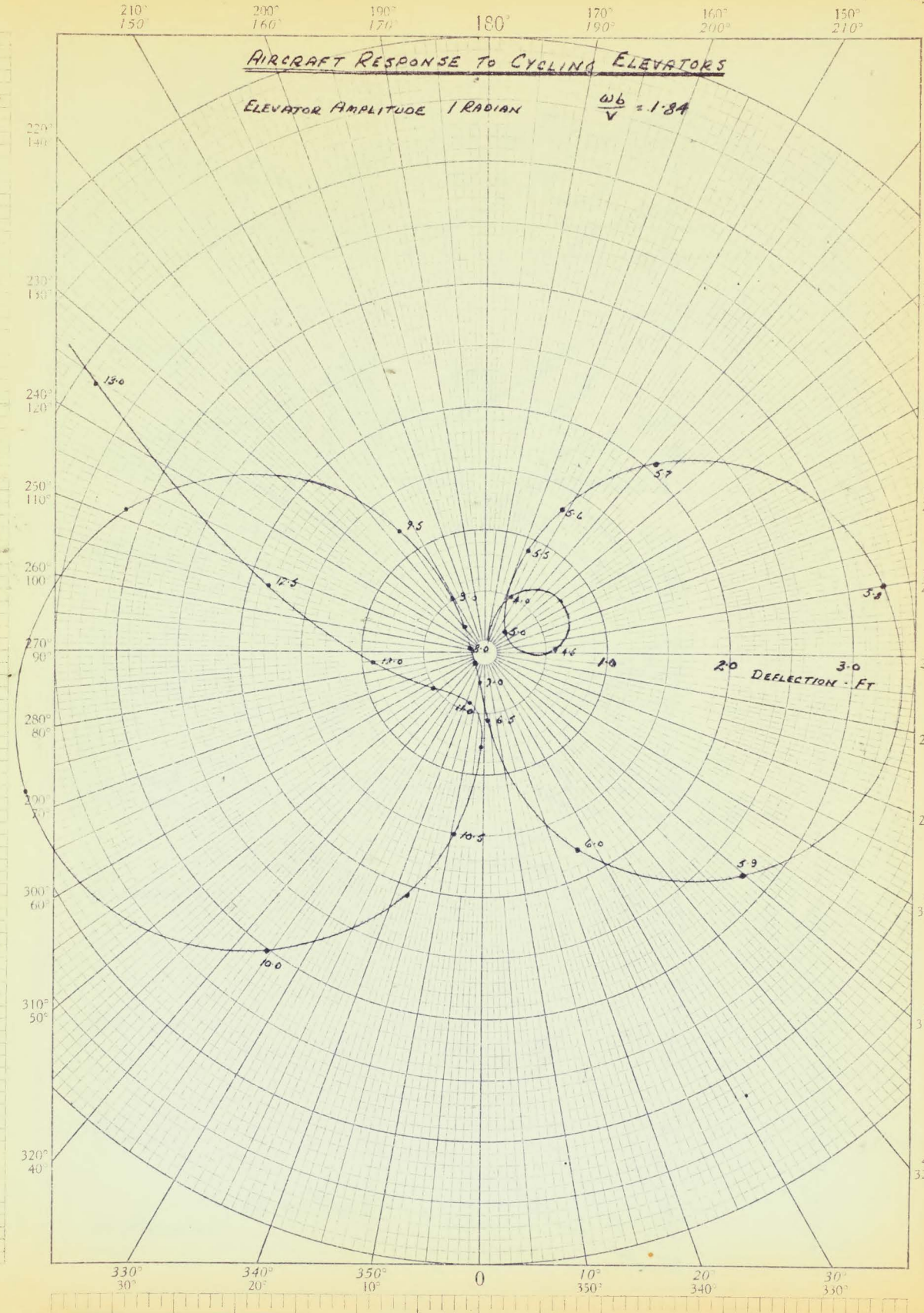

POLAR CO-ORDINATE 359-31
KEUFFEL & ESSER CO.
MADE IN U.S.A.

Fig. 21

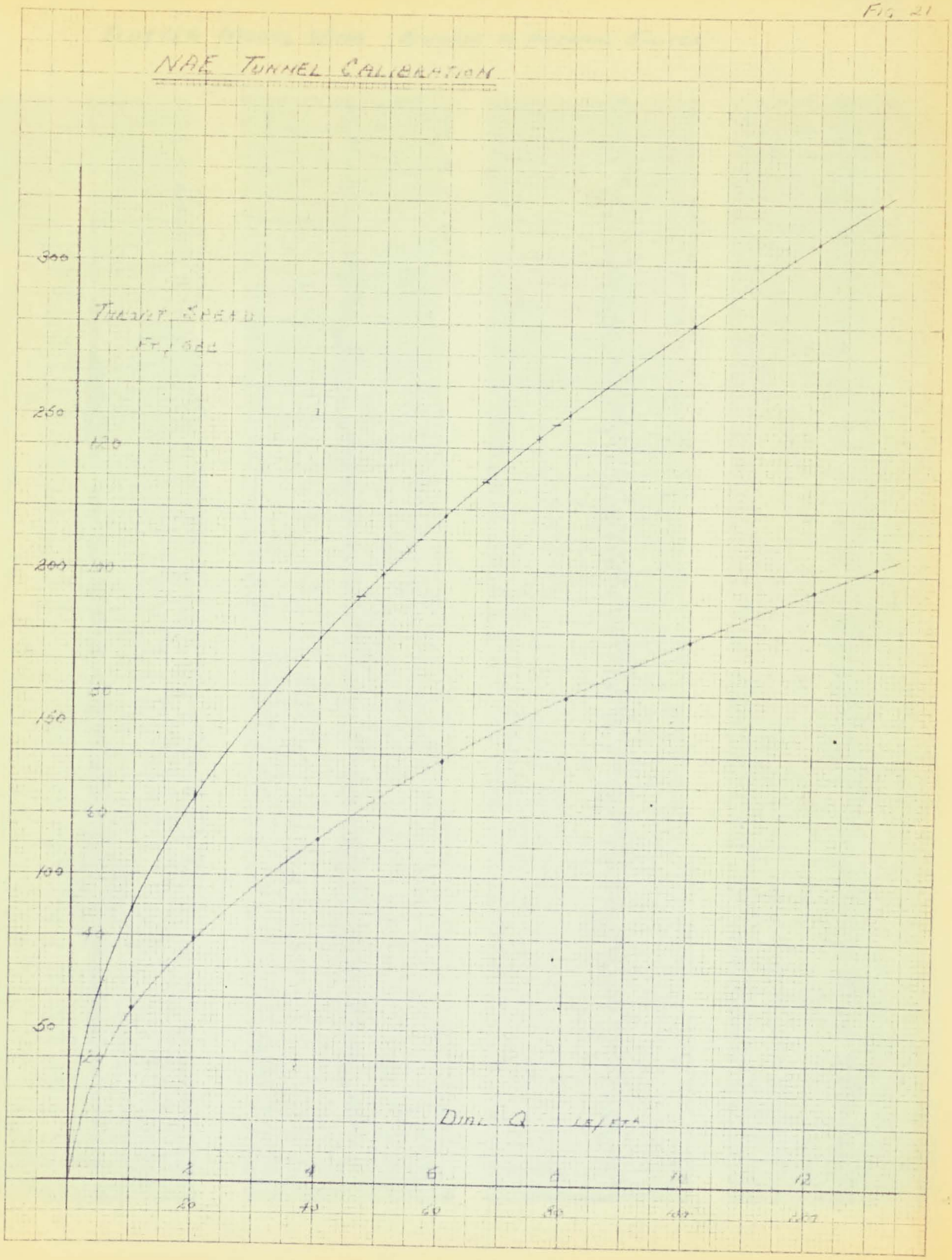

FIG 22

FLUTTER MODEL WING - RESPONSE TO INTERNAL EXCITER.

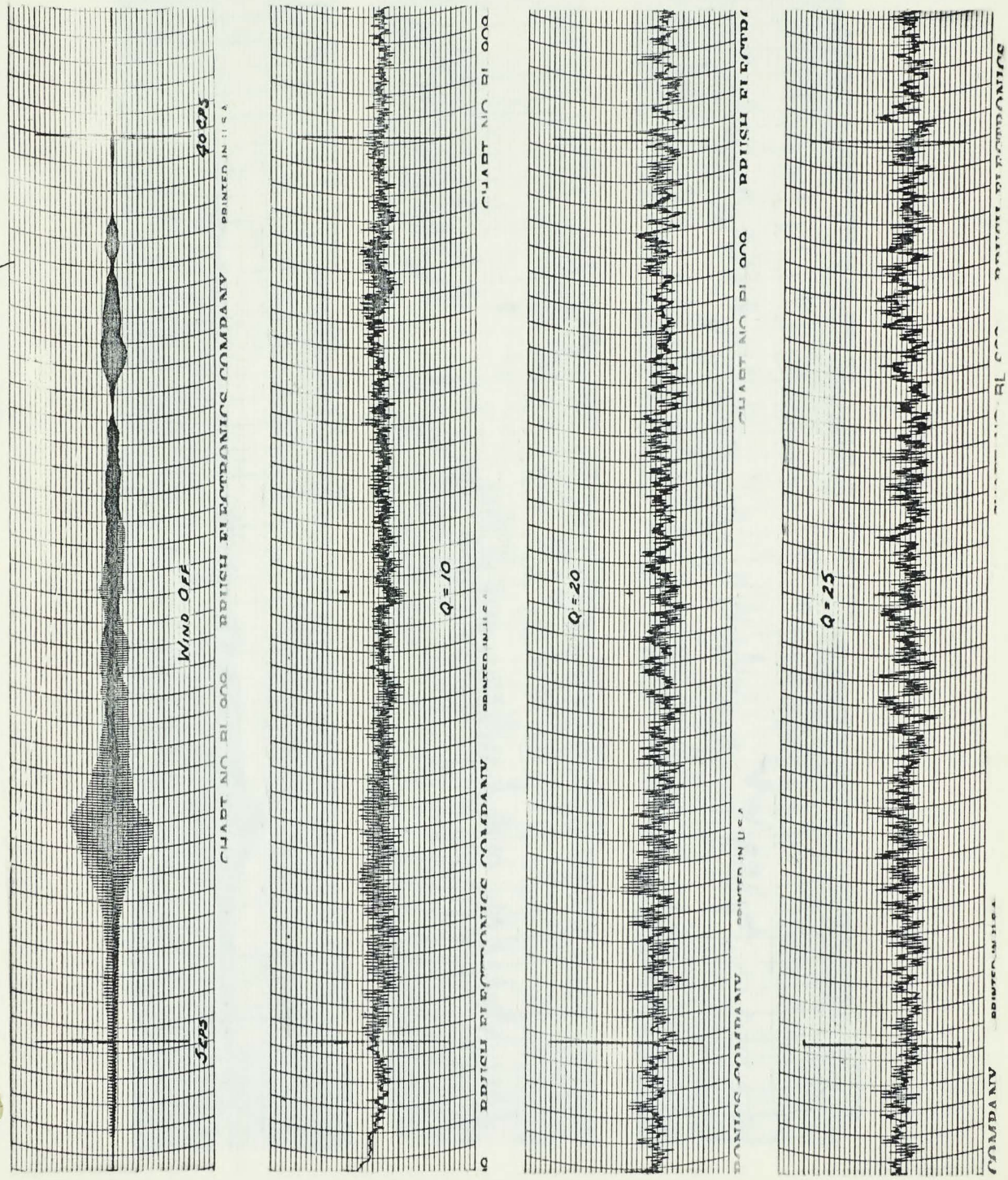

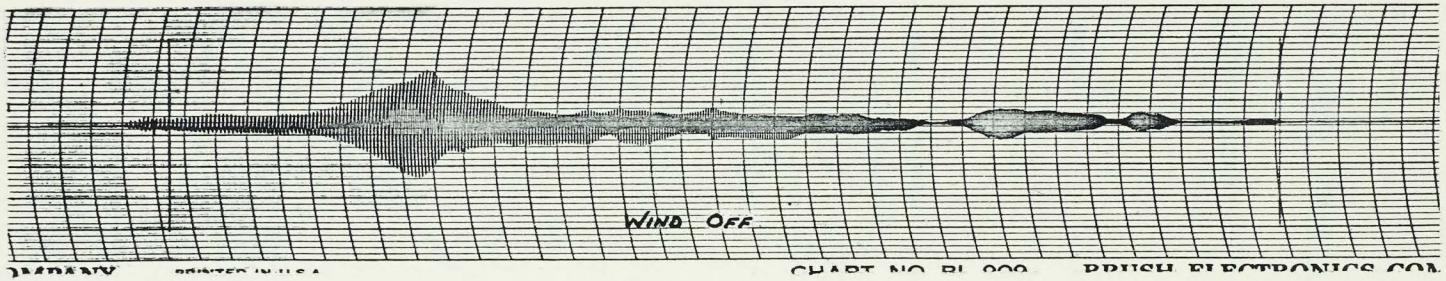
WIND OFF

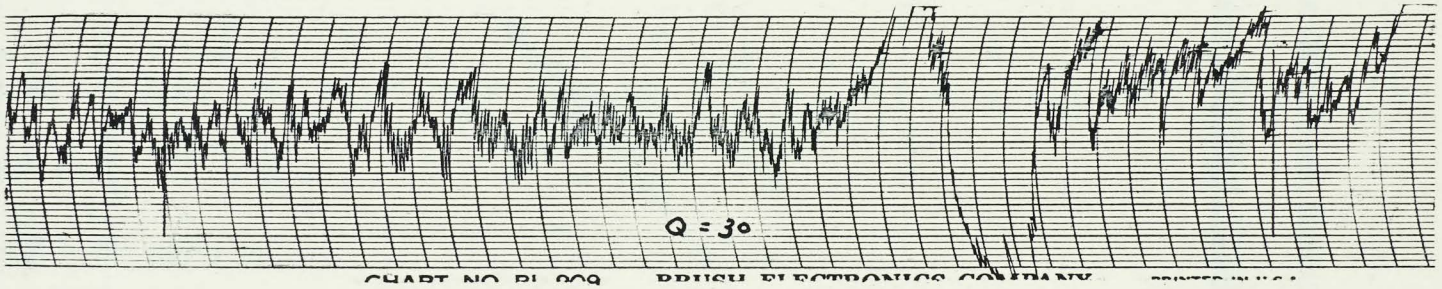
Q = 30

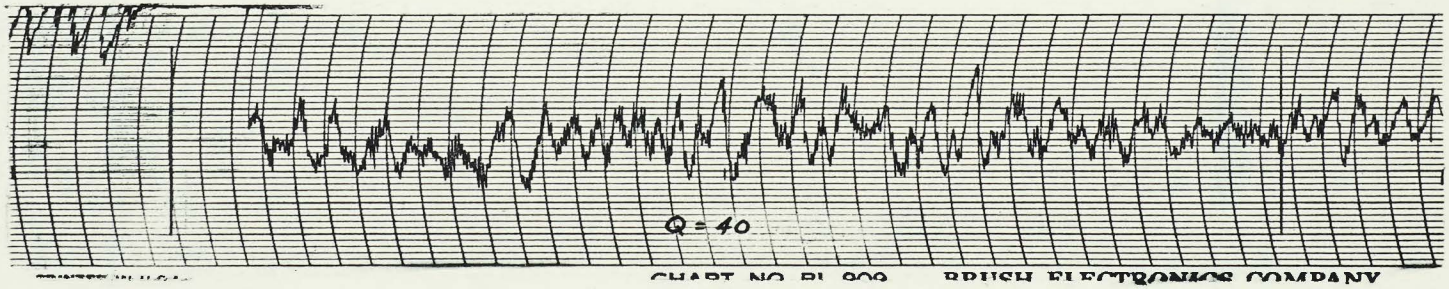
Q = 40